Novel combination of noninvasive morphological and solid-state characterization of drug-loaded core-shell electrospun fibers

Adrienn Kazsoki[1], Attila Farkas[2], Diána Balogh-Weiser[2,3], Elena Mancuso[4], Preetam K. Sharma[4], Dimitrios A. Lamprou[5], Romána Zelkó[1*]

[1]University Pharmacy Department of Pharmacy Administration, Semmelweis University, Hőgyes Endre utca 7-9, H-1092 Budapest, Hungary

[2]Department of Organic Chemistry and Technology, Budapest University of Technology and Economics, Műegyetem rakpart 3, H-1111 Budapest, Hungary

[3]Department of Physical Chemistry and Materials Science, Budapest University of Technology and Economics, Műegyetem rakpart 3, H-1111 Budapest, Hungary

[4]Nanotechnology and Integrated Bio-Engineering Centre (NIBEC), Ulster University, Jordanstown campus, UK

[5]School of Pharmacy, Queen's University Belfast, 97 Lisburn Road, Belfast, BT9 7BL, UK

Corresponding author*: Romána Zelkó, zelko.romana@pharma.semmelweis-univ.hu

ORCID:

Adrienn Kazsoki: 0000-0002-0611-3124; **Attila Farkas:** 0000-0002-8877-2587; **Diána Balogh-Weiser:** 0000-0002-9957-1203; **Elena Mancuso:** 0000-0003-1742-1656; **Preetam K. Sharma:** 0000-0002-5694-8445; **Dimitrios A. Lamprou** 0000-0002-8740-1661; **Romána Zelkó:** 0000-0002-5419-9137;

Keywords

coaxial electrospinning, core-shell electrospun fibers, drug delivery, Transmission electron microscopy, Raman spectroscopy

Chemical compounds studied in this article:

levofloxacin (PubChem CID: 149096); naproxen-sodium (PubChem CID: 23681059); polylactic acid (PubChem CID: 612); polyvinyl pyrrolidone (PubChem CID: 131751496); polysorbate 80 (PubChem CID: 5284448); hydroxypropyl-beta-cyclodextrin (PubChem CID:14049689); chloroform (PubChem CID: 6212); *N*,*N*-dimethylformamide (PubChem CID: 6228); ethanol (PubChem CID: 702)

Graphical abstract

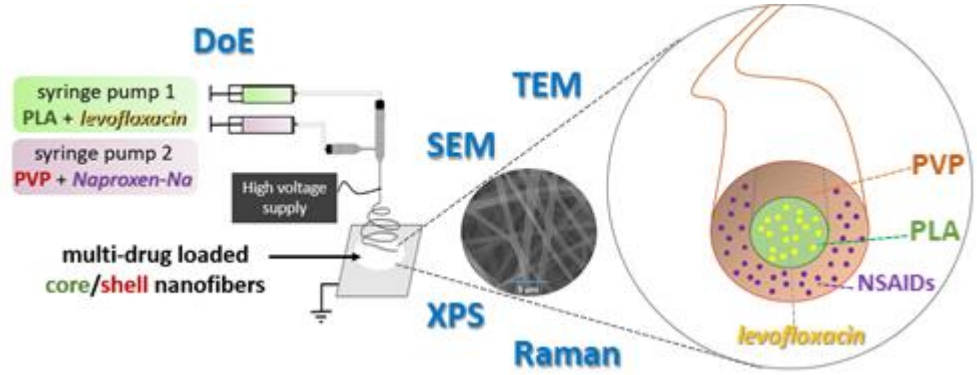

Abstract

Core-shell nanofibrous drug delivery systems have increasing attention in the last eyars due to their potential to incorporate two or more active pharmaceutical ingredients (APIs) individually into the desired layer (either core or sheath) and thus finely tune the release profile of even incompatible drugs in one system. This study aimed to formulate, and solid-state characterize levofloxacin-loaded polylactic acid (PLA) - naproxen-sodium-loaded polyvinyl pyrrolidone (PVP) bicomponent core-shell fibrous sheets and examined the electrospinnability of the precursor combinations. The selected drugs were of potential therapeutic relevance in similar systems that intended for wound healing, but in the present paper used as model drugs in order to understand the physicochemical properties of a drug loaded system. In order to determine the best core-and shell solution combination, a full factorial experimental design was used. The combination of various morphological (Scanning Electron Microscopy, Transmission Electron Microscopy) and microstructural characterization techniques (X-ray Photoelectron Spectroscopy and Raman spectroscopy) was applied in order to noninvasively obtain information about the structure of the fibers and the embedded drugs. The results indicated that core-shell fibers of different compositions were successfully prepared with various structural homogeneities. The best core-shell structure was obtained with 15% (w/w) shell concentration combined with 8 % (w/w) PLA solution concentration. Besides the conventional core-shell structural verification methods, a Raman spectroscopy method was implemented to reveal not only the core-shell structure of the PLA/PVP nanofibers, but the form of the embedded drugs, as well. The Raman mapping of the fibers confirm the above results and pointed out that as a results of the coaxial electrospinning process amorphous solid dispersion was formed.

1. Introduction

Electrospinning is a well controllable, relatively simple and cost-effective technique for the preparation of matrices with nano-and micrometer-sized fibers (Pelipenko et al., 2015; Smith and Ma, 2004; Xue et al., 2019). The unique properties of the fibrous materials, such as the high porosity with interconnected pore network and the increased surface area of the fibrous sheets, together with the active pharmaceutical ingredients (APIs) can be embedded into the polymeric matrix carrier in an amorphous state. These parameters could lead to an increased dissolution and thus provide bioavailability of drugs with lower solubility (Huang et al., 2003).

Due to nano- and microfibrous materials unique structure, the vast material variety, multifunction property and mass production, together with the formulation of nanofibrous scaffolds loaded with different drugs or drug combinations have been widely used as drug delivery systems for tissue engineering and wound bandage (Barnes et al., 2007; Haider et al., 2018). This materials widespread biomedical application lies its similar features and morphologies to the extracellular matrix, which is the non-cellular component presents within all tissues and organs, plays a crucial role in the wound healing process (Liu et al., 2017). Therefore, materials that can mimic their structure and can stimulate cell proliferation could help the wound healing (Rieger et al., 2013). Zahra et al., reported that a core–shell structure could provide a more controlled release of a model biocide with prolonged antibacterial properties than single nanofibers. These nanofibrous mats have the potential to selectively release antibacterial agents to prevent wound infections without delaying wound healing (Abdali et al., 2019).

However, the diverse field of applications required adequate functionality-related characteristics. In order to fulfil the increased quality and functionality requirement of the fibrous scaffolds, one of the emerging improvements is the development of a multicomponent core-shell fibrous structure, that can provide additional unique and essential properties that are relevant for biomedical applications (Elahi et al., 2013). The core polymer/composite can ensure features that are required for tissue regeneration. At the same time, the shell materials could preserve the unstable APIs embedded into the core from the unfavourable environmental effect, and can improve the hydrophilicity and the biocompatibility of the fibrous samples (Elahi et al., 2013; Han and Steckl, 2019). Besides that, one of the significant advantages of this core-shell nanostructures lies in the potential to tailor release properties of the incorporated drug, which is readily available with the careful choice of the drug-polymer-

solvent (or solvent mixture) precursor system (Huang and Thomas, 2018; Jiang et al., 2005). Basically, the core-shell fibrous structure can provide four directions to improve the polymer-based nanofibrous drug delivery systems (Han and Steckl, 2019):

(1) Combining two/three or more polymer and polymer-composition in a single fiber, which can provide the required biocompatibility and mechanical properties.

(2) With the drug incorporation into the core and covered by the shell, a sustained release of the drug can be achieved.

(3) There is the ability to incorporate two or more APIs individually into the desired layer (either core or sheath) and thus controlled release kinetics of the embedded drugs can be achieved.

(4) Trigger release: external stimuli-responsive controlled release is also feasible (Han and Steckl, 2019).

Although the bases of the production of core-shell type nanofibers are known in the literature, the development of a new core-shell system is still challenging. Even so, several drug combinations incorporated into the various polymer-based core-shell fibers; however, a core-shell structure verification technique has not been studied widely yet. A few studies are available, where the structure verification was investigated only with scanning electron microscopy (SEM) measurements (Huang and Thomas, 2018; Khalf et al., 2015). But it should be noted that, SEM can be a useful tool to verify the core-shell structure of the fibers, if the core component can be selectively extracted (Wang et al., 2010).

The typical and conventional core-shell structure characterization technique is the transmission electron microscopy (TEM), which is capable of detecting the materials with different densities. That is primarily applicable where different core- and shell material were used. However, it is also possible to make a core-shell fibrous sample using the same polymer as core and sheath materials. Still, in this case, this method is less applicable, which is due to the rather small difference in density caused by only the APIs (Alharbi et al., 2018; Chen et al., 2010; Pakravan et al., 2012; Sun et al., 2003; Zhang et al., 2004).

Atomic force microscopy (AFM) has also used to justify the structure, which applicability lies on the observation of the surface morphologies of single needle electrospun samples and the coaxial electrospun scaffold and even on the mechanomanipulation of the force spectroscopy. Still, for this measurement essential a sample of sparse surface coverage with least overlap between the fibers and only those part of the sample can be examined, that is totally lying on the disc (Chen et al., 2015; Kazsoki et al., 2018; Zander et al., 2011).

Another novel non-invasive technique is the Raman mapping, which can provide structural and quantitative information of the fibers by monitoring selective peaks of the polymers and the APIs (if their concentrations are big enough) – the technique is suitable for tracking the physical state of the embedded drugs (Farkas et al., 2015; Sfakis et al., 2017; Sharikova et al., 2020). However, due to its resolution limitation, it can be used effectively only in case of fibers with larger diameters (close or over micrometre size).

This study aimed to prepare levofloxacin-loaded polylactic acid (PLA) - naproxen-sodium-loaded poly(vinylpyrrolidone) (PVP) bicomponent core-shell fibrous sheets and examine the electrospinnability of the precursor combinations. The selected APIs have a potential therapeutic relevance in wound healing, but in the present paper, these molecules have been used as model drugs in order to understand the physicochemical properties of a drug-loaded core-shell fiber based system. A full factorial experimental design (of two factors in three levels) was used to determine the best combination of the drug-loaded core (PLA)-and shell (PVP) viscous solutions for coaxial electrospinning. The combination of conventional (as TEM and XPS) and novel morphological and solid-state characterization methods (like Raman spectroscopy) was applied to simultaneously monitor the core-shell structure and the form of actives embedded to the core and shell polymers. The studies performed in order to investigate the best composition with excellent fiber structure characteristic for potential application in chronic wound healing (**Fig. 1**).

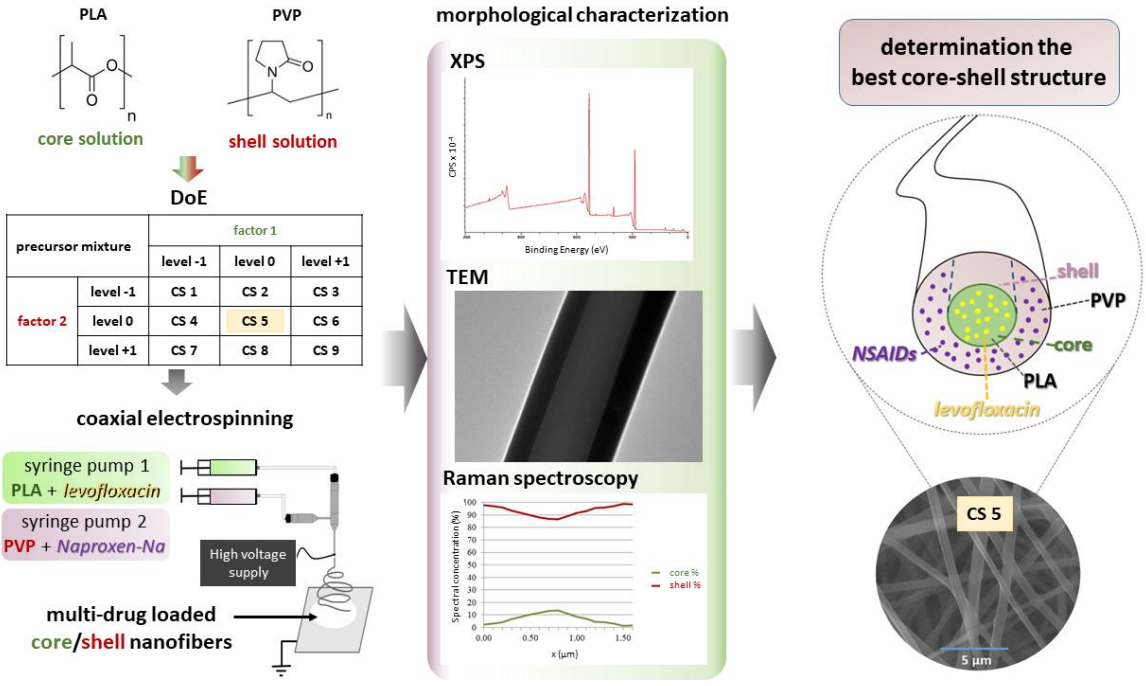

Fig. 1 Schematic representation of the steps and focus of the manuscript.

2. Materials and methods

2.1. Materials

Levofloxacin ((*S*)-9-fluoro-2,3-dihydro-3-methyl-10-(4-methylpiperazin-1-yl)-7-oxo-7*H*-pyrido[*1,2,3-de*]-1,4-benzoxazine-6-carboxylic acid) >98%, M=361.37 g mol^{-1}) and naproxen-sodium ((*S*)-6-Methoxy-α-methyl-2-naphthaleneacetic acid sodium salt, >98%, M=252.24 g mol^{-1}) were obtained commercially from Sigma-Aldrich (Budapest, Hungary) and were used as APIs. Polylactic acid (PLA, *GF45989881*, M_w~ 85000-160000 g mol^{-1} nominal granule size of 3-5 mm, density 1.24 g cm^{-3}) was chosen as the bases of the core part of the fibers, and poly(vinyl pyrrolidone) (PVP, Kollidon K90, average M_w~1500000 g mol^{-1}) was chosen for shell polymer, and both of them were obtained from Sigma-Aldrich (Budapest, Hungary). Hydroxypropyl-beta-cyclodextrin (average degree of substitution (n) ~4.5, (1135.0+ n*58.1) g mol^{-1}) was purchased from Cyclolab Ltd. (Budapest, Hungary). Polysorbate 80 was purchased from Molar Chemicals (Budapest, Hungary). Absolute ethanol (Molar Chemicals, Budapest, Hungary) and distilled water were used to prepare shell electrospinning precursor. As a solvent of the viscous solution of the core chloroform (anhydrous containing amylenes as stabilizers grade, >99%, Sigma Aldrich, Budapest, Hungary), and *N*,*N*-dimethylformamide (DMF, anhydrous grade 99,8%, Sigma Aldrich, Budapest, Hungary) were used. The materials were used without further purification.

2.2. Preparation of polymer precursors for electrospinning experiments

In this study, PLA and PVP were the chosen polymers for the core and sheath components, respectively.

Since the use of a precursor, solution has a significant impact on the success of the electrospinning process and the prepared samples morphology, preliminary experiments were done to determine the optimal composition of viscous polymer solutions for the shell and core formation. Therefore, the concentrations of the polymer solutions, the applied solvent mixture and other additives (the polysorbate 80) were determined.

For the shell solution water: ethanol 8:2 (m:m) and for the core solution chloroform: DMF 6:1 (m:m) solvent was used. The previous experimentation revealed that under 7% (w/w) PLA concentration, the single needle electrospinning did not result in bead-free, continuous fibers.

Naproxen-sodium-loaded PVP solutions and levofloxacin-loaded PLA solutions were prepared by using the appropriate amount of composition and solvent mixture under magnetic stirring until a clear, viscous solution was obtained. Both of the core and sheath solutions

were contained 0.5 % (w/w) polysorbate 80. The sheath solutions were containing 2 % (w/w) non-steroidal anti-inflammatory drug and 14 % (w/w) HP-β-CD. The levofloxacin concentration of the core solution was adjusted to 0.5 % (w/w).

A full factorial design of experiment was used to optimize fiber composition. The two factors were the core- and the shell polymer solution concentration and each of them was examined in three-level. Only the polymer concentration differed between the appropriate solutions. Based on the preliminary single-needle electrospinning experiments, the PLA concentration (factor 1) was chosen for 7, 8, 9 % (w/w), while 14, 15, 16 % (w/w) PVP concentration (factor 2) was examined (**Table 1)**.

Table 1 Design of experiments (DoE) by indicating the various electrospun samples

sample		**factor 1**		
		level -1	level 0	level +1
factor 2	level -1	CS_1	CS_2	CS_3
	level 0	CS_4	CS_5	CS_6
	level +1	CS_7	CS_8	CS_9

2.3. Coaxial electrospinning

Lab-scale coaxial electrospinning equipment (SpinSplit Ltd., Budapest, Hungary) was used for the fiber preparations. The homogenous precursor solutions were placed into plastic syringes (Luer lock syringe, Sigma Aldrich Ltd., Budapest, Hungary) that were connected to the conventional- (22 gauge) or coaxial emitter (inner needle gauge 22 and outer needle gauge 18) by teflon tubing. Pump systems provided the continuous feeding rate, which was 0.08 µl/s and 0.2 µl/s for core- and shell solution, respectively. The applied voltage was examined between 10-25 kV and the emitter to collector distance was set between 10-20 cm. Finally, the best fiber characteristic was achieved when 15±0.5 kV high voltage was applied, and the emitter to collector distance was set to 20 cm.

The samples were collected on a grounded aluminum plate covered with aluminum foil. During the electrospinning process, the Taylor cone formation and its stability were monitored by the camera system of the equipment, which support to identify best process parameters. The electrospinning experiments were performed in a well-controlled room at an ambient temperature of 22±1 °C with a relative humidity of 50±5 %.

2.4. Scanning electron microscopy (SEM)

The samples were fixed by a conductive double-sided carbon adhesive tape and then coated with a gold layer (JEOL JFC-1200 Fine Coater, JEOL Ltd., Tokyo, Japan). SEM images were

taken with a JEOL JSM-6380LA scanning electron microscope (JEOL Ltd., Tokyo, Japan). The acceleration voltage and the working distance were 15 kV and 10 mm, respectively.

2.5. Transmission Electron Microscope (TEM)

The core-shell structure of the coaxially electrospun nanofibers were examined on a JEOL JEM-2100F transmission electron microscope (TEM), operated at 200 kV. Samples for TEM analysis were prepared by directly depositing the as-spun nanofibers on a carbon grid (Agar Scientific) followed by fixing with a methanol drop. The TEM images were recorded using a charge-coupled device (CCD) camera controlled via Gatan DigitalMicrograph® software.

2.6. X-ray Photoelectron Spectroscopy (XPS)

In order to determine the chemical composition of the samples' surface (<5-10 nm), XPS measurements were carried out on a Kratos Axis Ultra instrument using Al $K_{\alpha 1}$ X-ray source ($h\upsilon$ = 1486.7 eV). The core-shell fibers electrospun onto aluminum foil were used for the XPS analysis. Wide energy survey scans (WESS) were performed for samples over the range of 0-1205 eV binding energy and pass energy of 160 kV.

A survey scan spectrum was taken, and the surface elemental compositions relative to carbon was calculated from the peak area with a correction for atomic sensitivity. The XPS spectra were analyzed using CasaXPS software. The quantification peaks were fitted using mixed Gaussian-Lorentzian (GL30) function after performing a Shirley background correction.

2.7. Raman microscopy measurements

The Raman spectroscopy measurements were carried out using LabRAM system (Horiba Jobin-Yvon, Lyon, France) coupled with an Olympus BX-40 optical microscope (Olympus, Hamburg, Germany) and with 532 nm Nd:YAG laser source (Sacher Lasertechnik, Marburg, Germany). For optical imaging, objectives of 20x and 100x magnifications were used.

A monochromator and Charge-Coupled-Device (CCD) detector were used for dispersion and detection of Raman photons, and during the measurements intensity filter (D=0.3) was applied. The data collected and processed using the Labspec 5 software.

During the measurements of reference samples (active pharmaceutical ingredients, polymers, cyclodextrin, and polysorbate), 20x objective was used. First, the spectra were collected over a more comprehensive spectral range of 100-2000 cm^{-1}, with that aim to select later the final measuring spectral range where most of the relevant signals of the fibrous samples can be detected. Finally, the spectral range of 346-1790 cm^{-1} was selected as the most suitable range

for data acquisition, and for this, a 1800 groove/mm optical grating was set to 1100 cm^{-1}. The resolution was 5 cm^{-1}. In the case of some components, fluorescence interference with different levels was observed, which was removed with baseline correction.

Remarkable differences were observed in the Raman activity between the individual components. While in the case of the crystalline drugs, 2 s acquisition time was sufficient to achieve ten thousand times intensities, while 8-30 s was required for the excipients to provide an excellent signal to noise ratio. For the measurements of the fibrous sample, an objective of 100x was used.

As for the Raman analysis, single fibers were suitable; the different nanofibrous samples (placebo-, and drug-loaded fibers) were electrospun for 3-4 s on a glass microscope slide covered by aluminum foil. These samples were investigated without any further sample preparation.

For the spatial distribution measurements, vertical fibers in the Y direction were chosen, which were monitored by the systematically moving of the motorized stage along in line in the X-direction. Each of the maps was collected with 0.1 µm step size. For the evaluation, the spectra of the placebo and drug-loaded fibers prepared by single-needle electrospinning were used.

The mapped spectra as well as the reference spectra corrected by fitting the linear baseline through specified points; all the spectra normalized by area.

3. Results and discussion

3.1 Morphological characterization

The SEM was used to investigate the morphology of the prepared sample by coaxial-electrospinning. SEM images of the electrospun samples showed that random orientated, clearly fibrous structure without beads and film-like elements were achieved with submicron fiber diameter sized (**Fig.2**). Remarkable differences could not be observed between the densities of the fibers in case of the core-shell fibrous samples electrospun from different precursor combinations.

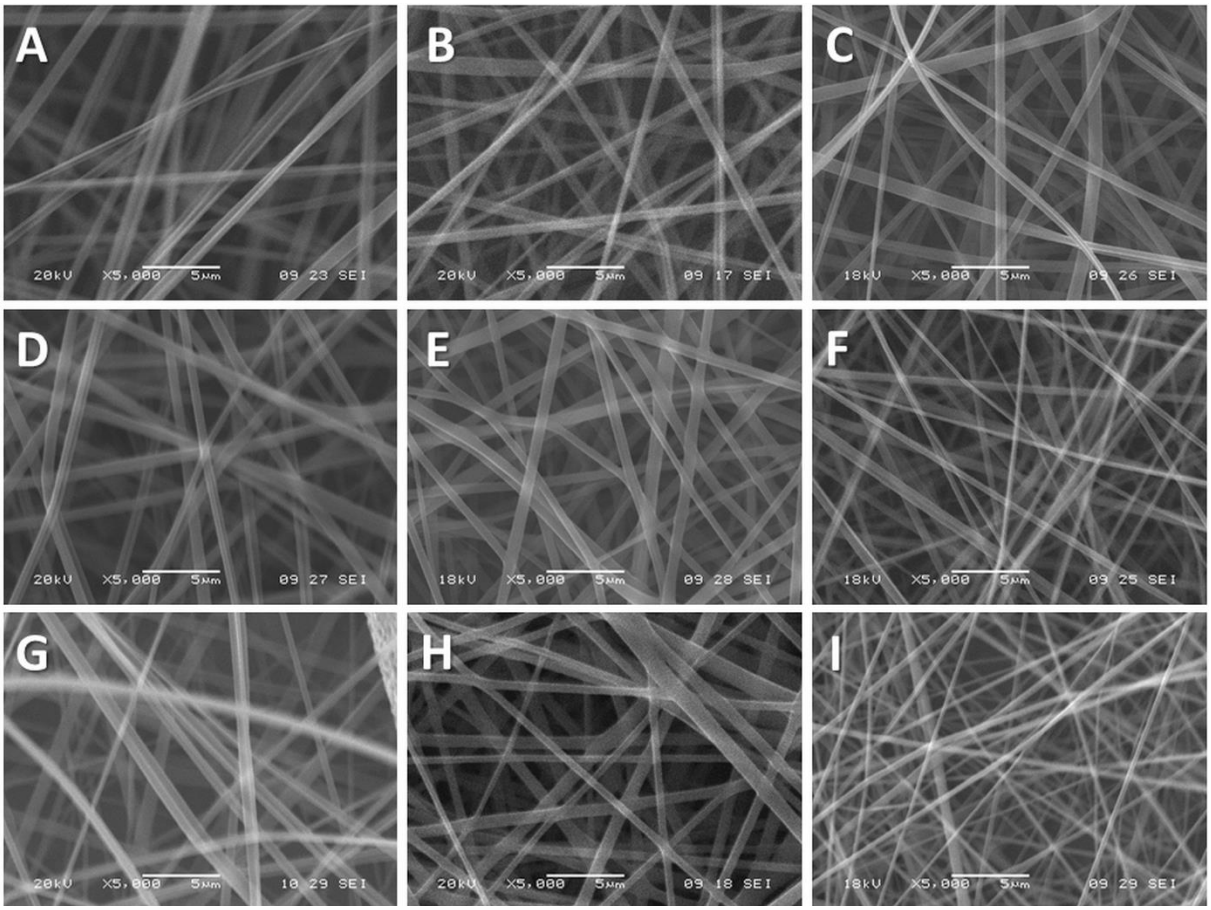

Fig. 2 SEM images of coaxially electrospun samples CS_1 (A), CS_2 (B), CS_3 (C), CS_4 (D), CS_5 (E), CS_6 (F), CS_7 (G), CS_8 (H) and CS_9 (I)

3.2 Structural investigation

The verification of the core-shell structure of the electrospun samples investigated by TEM measurements. **Fig. 3** shows the TEM micrographs of the core-shell structure of the composite ultrafine fibers. It was found that for the samples coded CS_4, CS_5, CS_6 and CS_7 (as can be seen in **Fig. 3 D, E, F, G** respectively), the diameter of the core structure was uniform throughout the fiber, evidencing a sharp core-shell interface for all the samples analysed. According to previous studies, this implies that the core and shell materials have different electron transmission ability (Zhang et al., 2006). In addition, the form of sharp boundaries is associated with the fast processing characteristic of electrospinning, preventing the mixing between the core solutions with the shell solution (Chen et al., 2010; Sun et al., 2006). For the samples based on 14% of PVP as well as for the 16% PVP with a core concentration of 8 and 9% PLA, the core-shell structure resulted irregular, with an evident effect on the resulting fiber morphology (**Fig. 3 A, B, C, H, I**). This could be attributed to the

fact that the core fluid jet out of coaxial capillaries might be split into a number of sub-jets during the electrospinning process (Xue et al., 2019).

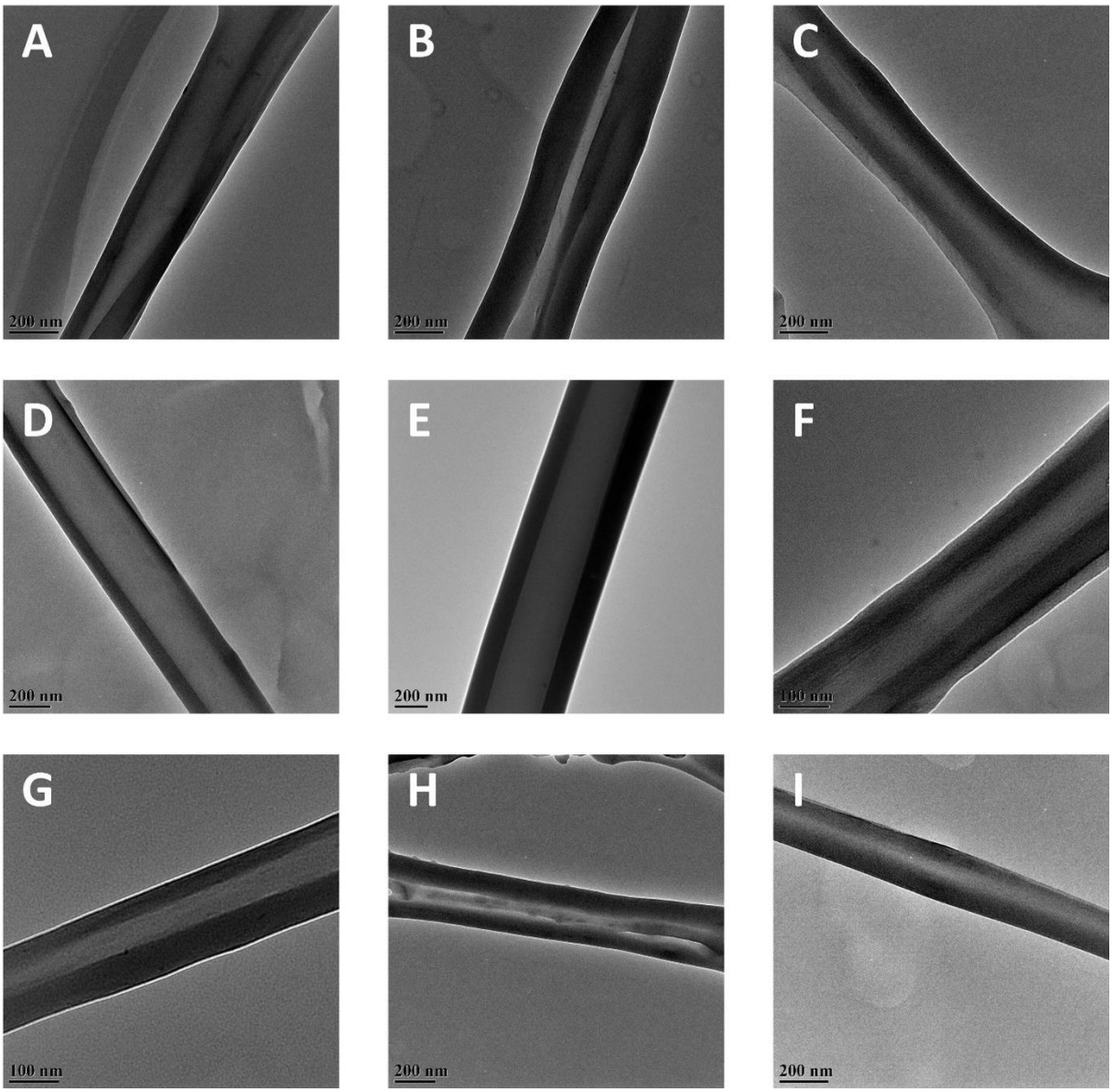

Fig. 3 TEM images of sample CS_1 (A), CS_2 (B), CS_3 (C), CS_4 (D), CS_5 (E), CS_6 (F), CS_7 (G), CS_8 (H) and CS_9 (I) coaxially electrospun samples

3.3 Surface characterization of the fibrous samples

The elemental composition on the surface of the PVP/PLA core-shell electrospun nanofiber characterized *via* XPS. In **Fig. 4** the WESS from all the core-shell samples are reported. As expected, the coaxial electrospun meshes showed very similar spectra across the different samples, characterized by four peaks corresponding to C1s (binding energy, 286 eV), N1s (binding energy, 400 eV), O1s (binding energy, 532 eV) and Na1s (binding energy, 1072 eV).

This suggests the consistent composition of the shell in all the samples. Moreover, the XPS data show no F and Cl signal on the PVP nanofiber surface. Since XPS elemental analysis can detect at the uppermost ~100 Å in-depth of an analyzed specimen (Sun et al., 2002). The absence of F 1s and Cl 2p peaks on the XPS spectra of the nanofiber surfaces indicates the following:

i) The shell thickness is at least beyond the ultimate detection depth of XPS (i.e., 5-10 nm).

ii) A good interfacial stability exists between the inner and the outer solution.

iii) Is an effective manufacturing electrospinning process (Sun et al., 2002).

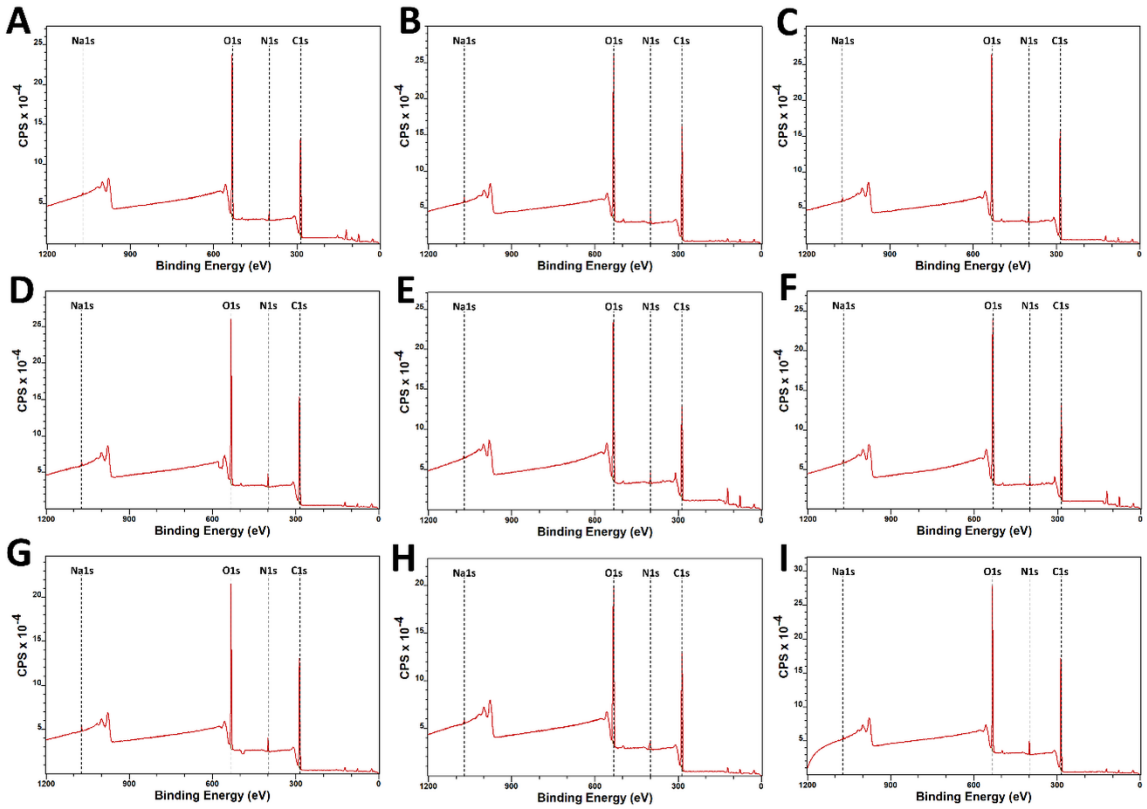

Fig. 4 XPS survey scan spectra from the coaxially produced nanofiber samples: CS_1 (A), CS_2 (B), CS_3 (C), CS_4 (D), CS_5 (E), CS_6 (F), CS_7 (G), CS_8 (H) and CS_9 (I) in 0-1200 eV range

3.4 Raman mapping

Besides the desired structure verification, investigation of the physical state of the embedded-drugs has a great impact on the drug delivery systems, because these affect the drug-release and the short- and long-term stability of the final dosage form. Raman mapping is a useful

mean to answer these questions. Based on the TEM results, the best three compositions were selected for further analysis of Raman spectroscopy, in which the effect of factor 1 can be examined.

Fig. 5 shows the Raman spectra of the active pharmaceutical ingredients, the placebo-and drug-loaded samples. Although in the case of the fibrous samples, lower intensities could be observed compared to the initial materials, the recorded spectra of the fibrous samples did not differ remarkably, suggesting that the fiber formations less influenced the shape of the spectra in the polymers.

It can be seen that there is a slight detectable difference between the spectra of crystalline drugs and drug-loaded fibers. In the latter cases, fewer and weaker drug signals can be observed. The broadening and merging of the spectra could be related to that the drugs incorporated into the fibers in an amorphous state. In the case of the levofloxacin-loaded fibrous sample, the most visible changing of the peak can see at 496, 518, 1555, 1621 and 1658 cm^{-1}, while the naproxen was contributed significantly more to the signals of the polymeric carrier at 523, 750, 1389, 1486, 1581 and 1634 cm^{-1}.

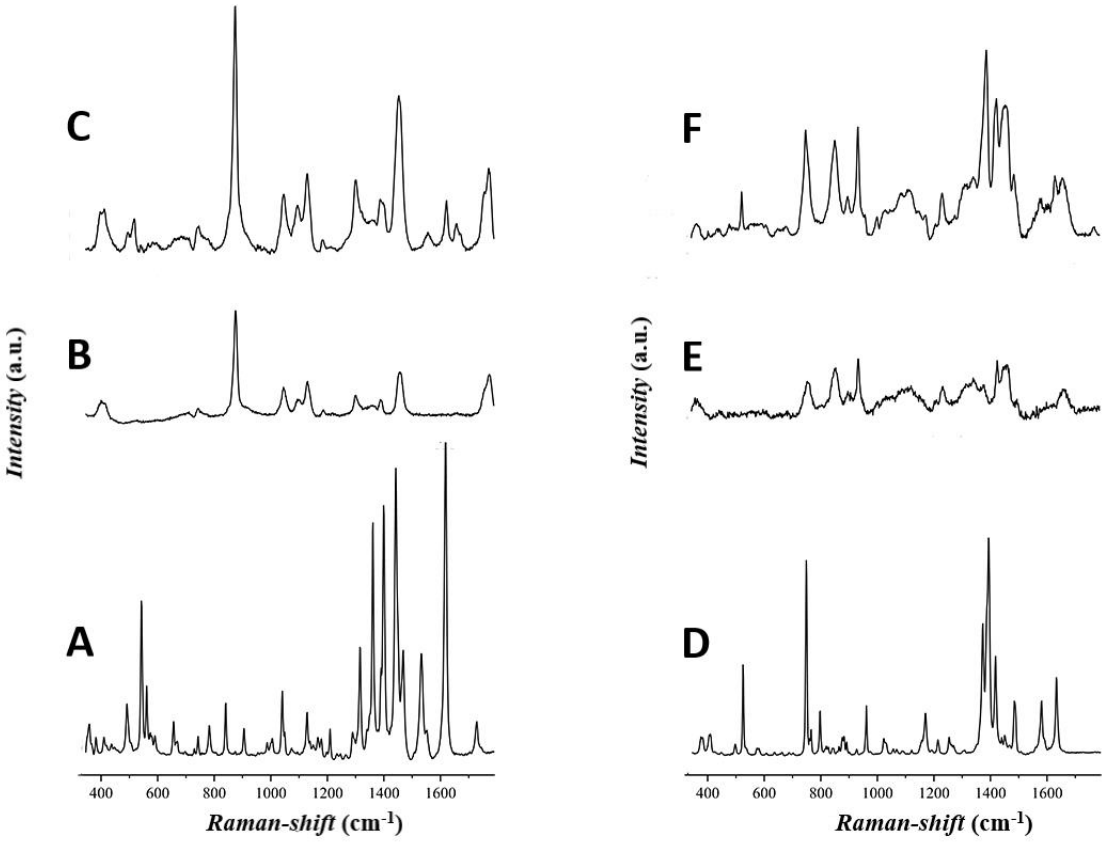

Fig. 5 Raman spectra of the model drugs, the placebo- and drug-loaded core- and shell nanofibers prepared by single-needle electrospinning: levofloxacin (A), placebo core

nanofiber (B), levofloxacin-loaded core nanofiber (C), naproxen-Na (D), placebo shell nanofiber (E), naproxen-Na-loaded shell nanofiber

A novel Raman mapping method was used to confirm the core-shell structure via the monitoring of the selective polymer signals of the spectra. For the evaluation, the single core and shell fiber reference spectra used and the spectral concentrations were calculated by classical least squares (CLS) method by using the total range of mentioned spectral range of 346-1790 cm^{-1}. ~~Because of very low concentration of active ingredient in core polymer, thus even lower in CS samples, the signal of PLA at 1770 cm^{-1} mainly indicated the appearance of the core.~~

The Raman maps are showing the polymer component contribution in the fibers (**Fig. 6**). The spectral concentration of the polymer components was normalized to 100%. The red line shows the spectral concentration of the core polymer (the PLA), while the red line represents the shell polymer (the PVP) concentration.

The signals from the edge of the fiber only came from the shell polymer, while the signals from the centre part (of the 2D projection of the fiber) included contributions from both of the used polymers, which is indicating the core-shell structure of the single coaxially electrospun fiber. This is consistent with the other results of the structural investigation methods.

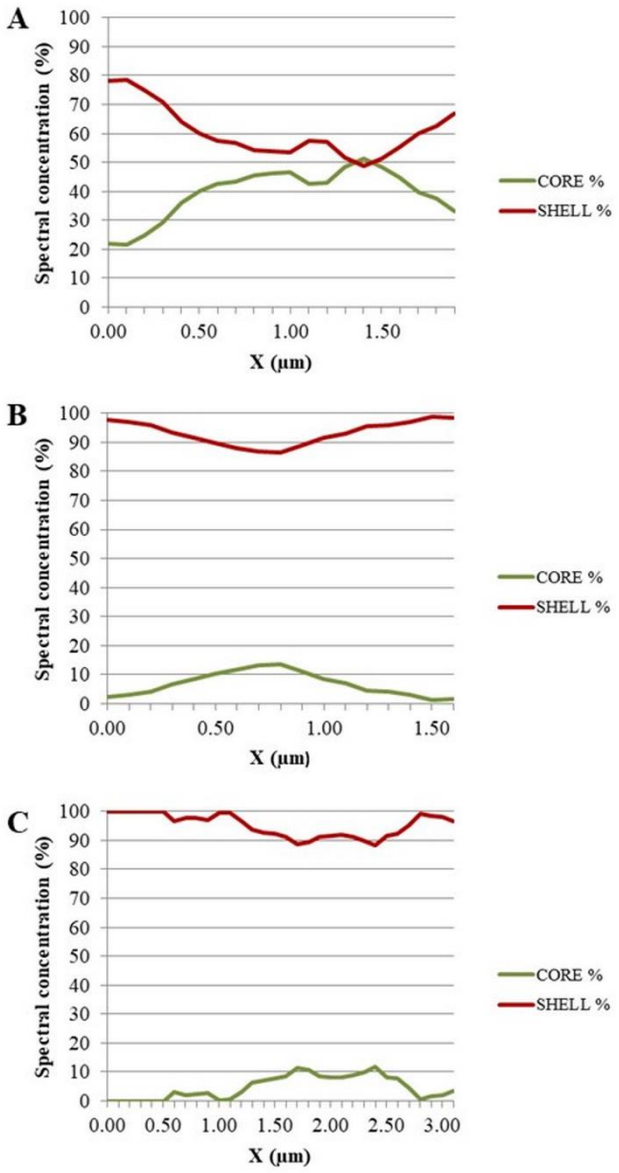

Fig. 6 Raman spectra from the core-shell fibrous samples (A:CS_4, B: CS_5, C:CS_6)

5. Conclusion

Levofloxacin-loaded polylactic acid (PLA) - naproxen-sodium-loaded poly(vinylpyrrolidone) (PVP) bicomponent core-shell fibrous sheets were formulated from precursors of different concentrations according to a full factorial DoE to optimize the fiber composition. The SEM measurements indicated that each of the nine examined core-shell precursor combinations enabled the formation of clear fibrous mats. The set of the conventional fiber structure characterization (e.g. TEM) indicated that core-shell fibers of different compositions were successfully prepared with various structural homogeneities. The XPS spectra of the nanofiber surfaces indicated that there is excellent interfacial stability between the inner and

outer polymer solution. The best sample was achieved with 15% (w/w) shell concentration combined with 8 % (w/w) PLA solution concentration. Besides the conventional core-shell structural verification methods, a Raman spectroscopy method was applied successfully to reveal the core-shell structure of the PLA/PVP nanofibers, since the spatial distributions of the polymers were found to be different in the sampling points; moreover, it was also pointed out that amorphous solid dispersions were formed.

The core-shell fibrous materials have been successfully prepared in the literature using numerous polymer combinations; however, there is no universal morphological characterization method for structure verifications. With regard to the characterization of the structure of the coaxially electrospun samples the properties of the used polymers are a major consideration that should be considered when selecting characterization methods. A combination of several methods may be required to obtain information about the structure. Even with its limitation, the Raman mapping could be a universal method for the fiber structure determination, all the more so as it can obtain information about the distribution of the drug if the concentration of embedded drugs is large enough in the fibers. The latter could be the subject of future research.

6. Declarations

6.1. Funding

This project was supported by ÚNKP-19-3-I New National Excellence Program of the Ministry for Innovation and Technology.

6.2. Conflict of interest disclosure

The authors declare no conflict of interest.

6.3. Availability of data and material

Not applicable.

6.4. Code availability

Not applicable.

6.5. Authors' Contributions

Adrienn Kazsoki designed the experiments and accomplished the viscous solution preparation and formulated the electrospun fibrous mats. Analyzed and evaluated the measurements and wrote the manuscript. *Attila Farkas* performed and evaluated the Raman spectroscopy measurements. *Elena Mancuso, Preetam K. Sharma, Dimitrios A. Lamprou* performed the TEM and XPS measurements and analysis. *Diána Balogh-Weiser* performed the SEM measurements. *Romána Zelkó* finalized the manuscript.

References

Abdali, Z., Logsetty, S., Liu, S., 2019. Bacteria-Responsive Single and Core–Shell Nanofibrous Membranes Based on Polycaprolactone/Poly(ethylene succinate) for On-Demand Release of Biocides. ACS Omega 4, 4063-4070.

Alharbi, H.F., Luqman, M., Khalil, K.A., Elnakady, Y.A., Abd-Elkader, O.H., Rady, A.M., Alharthi, N.H., Karim, M.R., 2018. Fabrication of core-shell structured nanofibers of poly (lactic acid) and poly (vinyl alcohol) by coaxial electrospinning for tissue engineering. European Polymer Journal 98, 483-491.

Barnes, C.P., Sell, S.A., Boland, E.D., Simpson, D.G., Bowlin, G.L., 2007. Nanofiber technology: Designing the next generation of tissue engineering scaffolds. Advanced Drug Delivery Reviews 59, 1413-1433.

Chen, R., Huang, C., Ke, Q., He, C., Wang, H., Mo, X., 2010. Preparation and characterization of coaxial electrospun thermoplastic polyurethane/collagen compound nanofibers for tissue engineering applications. Colloids and Surfaces B: Biointerfaces 79, 315-325.

Chen, Y., Qian, C., Miao, N., 2015. Atomic force microscopy indentation to determine mechanical property for polystyrene–silica core–shell hybrid particles with controlled shell thickness. Thin Solid Films 579, 57-63.

Elahi, M.F., Lu, W., Guopling, G., Khan, F., 2013. Core-shell Fibers for Biomedical Applications- A Review. Journal of Bioengineering & Biomedical Science.

Farkas, A., Vajna, B., Sóti, P.L., Nagy, Z.K., Pataki, H., Van der Gucht, F., Marosi, G., 2015. Comparison of multivariate linear regression methods in micro-Raman spectrometric quantitative characterization. Journal of Raman Spectroscopy 46, 566-576.

Haider, A., Haider, S., Kang, I.-K., 2018. A comprehensive review summarizing the effect of electrospinning parameters and potential applications of nanofibers in biomedical and biotechnology. Arabian Journal of Chemistry 11, 1165-1188.

Han, D., Steckl, A.J., 2019. Coaxial Electrospinning Formation of Complex Polymer Fibers and their Applications. ChemPlusChem 84, 1453-1497.

Huang, C., Thomas, N.L., 2018. Fabricating porous poly(lactic acid) fibres via electrospinning. European Polymer Journal 99, 464-476.

Huang, Z.-M., Zhang, Y.Z., Kotaki, M., Ramakrishna, S., 2003. A review on polymer nanofibers by electrospinning and their applications in nanocomposites. Composites Science and Technology 63, 2223-2253.

Jiang, H., Hu, Y., Li, Y., Zhao, P., Zhu, K., Chen, W., 2005. A facile technique to prepare biodegradable coaxial electrospun nanofibers for controlled release of bioactive agents. Journal of Controlled Release 108, 237-243.

Kazsoki, A., Szabó, P., Domján, A., Balázs, A., Bozó, T., Kellermayer, M., Farkas, A., Balogh-Weiser, D., Pinke, B., Darcsi, A., Béni, S., Madarász, J., Szente, L., Zelkó, R., 2018.

Microstructural Distinction of Electrospun Nanofibrous Drug Delivery Systems Formulated with Different Excipients. Molecular Pharmaceutics 15, 4214-4225.

Khalf, A., Singarapu, K., Madihally, S.V., 2015. Cellulose acetate core–shell structured electrospun fiber: fabrication and characterization. Cellulose 22, 1389-1400.

Liu, M., Duan, X.-P., Li, Y.-M., Yang, D.-P., Long, Y.-Z., 2017. Electrospun nanofibers for wound healing. Materials Science and Engineering: C 76, 1413-1423.

Pakravan, M., Heuzey, M.-C., Ajji, A., 2012. Core–Shell Structured PEO-Chitosan Nanofibers by Coaxial Electrospinning. Biomacromolecules 13, 412-421.

Pelipenko, J., Kocbek, P., Kristl, J., 2015. Critical attributes of nanofibers: Preparation, drug loading, and tissue regeneration. International Journal of Pharmaceutics 484, 57-74.

Rieger, K.A., Birch, N.P., Schiffman, J.D., 2013. Designing electrospun nanofiber mats to promote wound healing – a review. Journal of Materials Chemistry B 1, 4531-4541.

Sfakis, L., Sharikova, A., Tuschel, D., Costa, F.X., Larsen, M., Khmaladze, A., Castracane, J., 2017. Core/shell nanofiber characterization by Raman scanning microscopy. Biomed. Opt. Express 8, 1025-1035.

Sharikova, A., Foraida, Z.I., Sfakis, L., Peerzada, L., Larsen, M., Castracane, J., Khmaladze, A., 2020. Characterization of nanofibers for tissue engineering: Chemical mapping by Confocal Raman microscopy. Spectrochimica Acta Part A: Molecular and Biomolecular Spectroscopy 227, 117670.

Smith, L.A., Ma, P.X., 2004. Nano-fibrous scaffolds for tissue engineering. Colloids and Surfaces B: Biointerfaces 39, 125-131.

Sun, B., Duan, B., Yuan, X., 2006. Preparation of core/shell PVP/PLA ultrafine fibers by coaxial electrospinning. Journal of Applied Polymer Science 102, 39-45.

Sun, Y., Yin, Y., Mayers, B.T., Herricks, T., Xia, Y., 2002. Uniform Silver Nanowires Synthesis by Reducing AgNO3 with Ethylene Glycol in the Presence of Seeds and Poly(Vinyl Pyrrolidone). Chemistry of Materials 14, 4736-4745.

Sun, Z., Zussman, E., Yarin, A.L., Wendorff, J.H., Greiner, A., 2003. Compound Core–Shell Polymer Nanofibers by Co-Electrospinning. Advanced Materials 15, 1929-1932.

Wang, C., Yan, K.-W., Lin, Y.-D., Hsieh, P.C.H., 2010. Biodegradable Core/Shell Fibers by Coaxial Electrospinning: Processing, Fiber Characterization, and Its Application in Sustained Drug Release. Macromolecules 43, 6389-6397.

Xue, J., Wu, T., Dai, Y., Xia, Y., 2019. Electrospinning and Electrospun Nanofibers: Methods, Materials, and Applications. Chemical Reviews 119, 5298-5415.

Zander, N.E., Strawhecker, K.E., Orlicki, J.A., Rawlett, A.M., Beebe, T.P., 2011. Coaxial Electrospun Poly(methyl methacrylate)–Polyacrylonitrile Nanofibers: Atomic Force

Microscopy and Compositional Characterization. The Journal of Physical Chemistry B 115, 12441-12447.

Zhang, Y., Huang, Z.-M., Xu, X., Lim, C.T., Ramakrishna, S., 2004. Preparation of Core−Shell Structured PCL-r-Gelatin Bi-Component Nanofibers by Coaxial Electrospinning. Chemistry of Materials 16, 3406-3409.

Zhang, Y.Z., Wang, X., Feng, Y., Li, J., Lim, C.T., Ramakrishna, S., 2006. Coaxial Electrospinning of (Fluorescein Isothiocyanate-Conjugated Bovine Serum Albumin)-Encapsulated Poly(ε-caprolactone) Nanofibers for Sustained Release. Biomacromolecules 7, 1049-1057.